

Experimental Studies of RF Generated Ionospheric Turbulence

J. P. Sheerin¹; N. Watanabe¹; N. Rayyan¹; B. J Watkins²; W. A. Bristow²;

¹Department of Physics and Astronomy

Eastern Michigan Univ.

Ypsilanti, MI 48197

U.S.A.

²Geophysical Institute

U. Alaska-Fairbanks

Fairbanks, AK 99775

U.S.A.

ABSTRACT

The high power HAARP HF transmitter is employed to generate and study strong Langmuir turbulence (SLT) in the interaction region of overdense ionospheric plasma. Diagnostics included the Modular UHF Ionospheric Radar (MUIR) sited at HAARP, the Super-DARN Kodiak HF radar, and HF receivers to record stimulated electromagnetic emissions (SEE). Dependence of diagnostic signals on HAARP HF parameters, including pulse length, duty cycle, aspect angle, and frequency were recorded. Short pulse, low duty cycle experiments demonstrate control of artificial field-aligned irregularities (FAI) and isolation of ponderomotive effects. For the first time, simultaneous multi-angle radar measurements of plasma line spectra are recorded demonstrating marked dependence on aspect angle with the strongest interaction region observed displaced southward of the HF zenith pointing angle. For a narrow range of HF pointing between Spitz and magnetic zenith, a reduced threshold for FAI is observed. High time resolution studies of the temporal evolution of the plasma line reveal the appearance of an overshoot effect on ponderomotive timescales. Numerous measurements of the outshifted plasma line are observed. Experimental results are compared to previous high latitude experiments and predictions from recent modeling efforts.

1. INTRODUCTION

Transmission of high power HF (2 – 10 MHz) waves into the Earth's ionosphere is known to increase the electron temperature, and generate a large number of nonlinear phenomena including plasma turbulence. When the frequency of the HF wave, called the pump wave, is lower than the local plasma frequency of the ionosphere, $\omega < \omega_p$, the wave number k becomes imaginary. Hence the HF wave decays in the ionosphere (*Walker, 1979*) and couples to high-frequency electron plasma waves, which are called Langmuir waves (LW), and low frequency ion waves, which are called ion-acoustic waves (IAW). This primary mechanism is called the Parametric Decay Instability (PDI) (*DuBois, et al. 2001*). The group velocity of the HF pump wave tends to zero upon approach to the reflection height and the wave electric field becomes parallel to the geomagnetic field. Consequently, the HF pump waves generate parametric instabilities just below the reflection height. The Langmuir waves, produced by PDI, can decay into another LW and another IAW if their amplitudes exceed a threshold. This second decay process is called Langmuir Decay, and the excitation of the instability is called Langmuir Decay Instability (LDI). The LW accelerates electrons, and which can produce intense optical emissions. The decay of waves continues until the threshold for the decay is no longer exceeded.

Langmuir turbulence occurs typically between the matching height and the reflection height (*Isham et al. 1999*). It has been observed that an HF pump frequency that is slightly below the critical frequency and close to the third gyro-frequency generated can effectively generate Langmuir Turbulence.

The aspect angle of the HF pump wave strongly affects the above mentioned processes resulting from heating of the ionosphere (*Rietveld et al. 2003*). When the HF pump wave angle is between the Spitze angle and the magnetic zenith angle, a strong enhancement of the parametric decay has been observed. The Spitze angle is shown in equation (1) (*Ashrafi et al. 2007*) and describes the range of angles for which an O-mode pump wave can propagate to the highest reflection altitude (*Isham et al. 2005*). On the other hand, an O-mode pump wave incident with an angle larger than the Spitze angle reflects before reaching the highest altitude.

$$\text{Spitze angle} = \arcsin \left(\left[\left(\frac{Y}{1+Y} \right) \right]^{\frac{1}{2}} \sin \theta_B \right) \quad (1)$$

where $Y = f_b / f_0$, f_b is frequency of the gyro-cyclotron frequency, f_0 is frequency of the HF pump wave, and θ_B is magnetic zenith angle. Electron temperature strongly increases with the HF pump wave at or close to the magnetic zenith angle (*Rietveld et al. 2003*). The features of electron enhancement are different for different duty cycles of the HF pump wave. Thermal and density perturbations are moderated with a low duty cycle, since the bulk heating effect becomes small (*Cheung, et al. 1997*).

If the pump electric field amplitude is sufficient, Langmuir cavitons can be formed, which are localized density depressions and electric field maxima. This process is referred to as strong Langmuir turbulence (SLT). Observationally, incoherent radar observations of spectrum features known as cascade, collapse, coexistence of cascade and collapse, and outshifted plasma line (OPL) predict the existence of SLT. Cascade refers to the spectral feature of the PDI and LDI lines. The cascade is observed at or below the PDI matching height. The first cascade line shows the “mother” LW due to PDI, and the other cascade lines show “daughter” LWs due to LDI. The cascade lines in a spectral sideband may be only odd multiples of the LW frequencies. The process of cascading continues as long as subsequent daughter waves exceed the threshold. The electron and ion temperature affect the spectral width of the cascade, and the total spectral power is proportional to the electron density (*Forme and Fontaine, 1999*).

The collapse line is the spectral feature corresponding to the collapse of the Langmuir cavitons which occurs near the reflection height of the HF pump wave (*DuBois, et al. 1995*). The collapsing cavitons are density cavities, which have the size of approximately ten of meters and are created by the ponderomotive pressure (intensity) of electromagnetic waves (*Fejer, et al., 1983*). Strong Langmuir Turbulence (SLT) is considered to be driven by collapsing cavitons (*Sheerin, et al., 1982; Isham et al. 2003*). The density cavity is deepened by the ponderomotive pressure, and which intensifies the localized field. Nonlinear steepening of the trapped field leads to collapse. Caviton collapse dissipates most of the electrostatic energy through interaction with electrons (*DuBois et al., 1991*). Moreover, *DuBois et al. (1991)* describe that the process of collapse is apparent for approximately a microsecond after switch-off of the pump wave. Caviton collapse has been observed during the HF heating (*Duncan and Sheerin, 1985*). The cavitons were formed near the reflection height of the HF pump wave (*Sheerin et al. 1982*). The coexistence of the cascade and collapse appears around the PDI matching height (*Hanssen et al. 1992, DuBois et al. 1991 and 1993*).

The outshifted plasma lines (OPL) in the spectrum refers to LW's which appear at frequency shifts above the HF pump wave frequency shift (*Isham et al. 1996*). OPL signifies the presence of LWs with large frequencies that are generated by the accelerated electrons which in turn is related to collapse. Langmuir turbulence is observed at the UHF matching height where the wave vector of the

HF pump wave is twice as much as the wave vector of the UHF wave which is called the Bragg scatter condition. In this paper we describe results of experiments investigating the generation of RF generated turbulence as function of aspect angle of the HF pump wave, pulselength, HF duty cycle, and related parameters.

2. EXPERIMENTS

Experiments to investigate excitation of Strong Langmuir Turbulence (SLT) and plasma instabilities as a function of aspect angle were carried out at the High Frequency Active Auroral research program (HAARP) facility in Gakona Alaska (latitude 62.39° N and longitude 145.15° W), over the course of several campaign days in the summers of 2010 - 2012. The HF transmitter power of the 3.6 MW (EPR 88.8 – 91 dBW) ionospheric heater was transmitted into the F2 region of the ionosphere with O-mode polarization and frequency chosen just to be below the f_oF2 -critical frequency based on ionosonde observations. The typical HF pointing angles were 7° , 11° , and 14° southward with respect to vertical as shown in Figure 1. The magnetic declination at HAARP is approximately 15° . The HF transmission schedule typically consisted of a 60 ms pulse, in a 12 sec IPP giving a duty cycle of 0.5 %. The format is repeated for a 5 min sequence (4 min pulsing and 1 min off). The very low duty cycle was used to avoid the creation of artificial field aligned irregularities that occurs under prolonged bulk heating of the plasma, thus observations are dominated by more rapid SLT processes. The Modular UHF Ionospheric Radar (MUIR) located at HAARP facility was used for observations of parametric decay of the HF pump wave. The frequency of the transmission of MUIR is 446 MHz. MUIR sends and receives the backscattered wave of the radar pulse, and it can detect LW and IAW. The pointing angle of the UHF MUIR signal was also varied at 6° , 12° , and 15° . Since the UHF IPP is only 3 msec, and the MUIR radar can change pointing pulse-to-pulse, the MUIR radar is able to diagnose each 60 msec HF pulse almost simultaneously at the 3 different UHF angles. The time delay between the UHF transmission and receiving the backscatter echo provides the reflection height. The difference between the frequency MUIR transmits and the frequency MUIR receives is close to the HF pump frequency (*Sheerin, et al. 2003*). The backscatter spectrum shows cascade lines that are observed LWs. The spectrum shows only upshifted plasma lines that are cascade lines of odd multiples of LWs as discussed above. A schematic of the HF pump transmission and MUIR diagnostic geometry are shown in Fig 1.

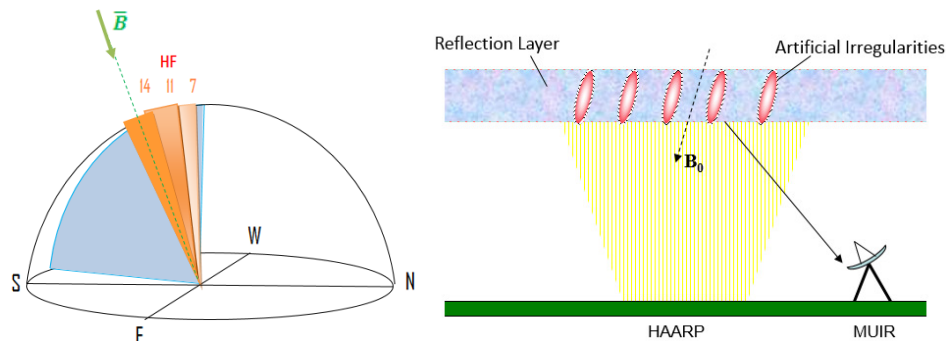


Fig 1. (Left) Schematic of HF transmission directed southward with HF pointing angle of 7° - 11° - 14° from vertical. (Right) Schematic of HF transmission and diagnostics for the observation provided by the MUIR (Modular UHF Ionospheric Radar) at HAARP, Gakona, Alaska.

3. OBSERVATIONS

For all HF pointing angles, 7° , 11° , and 14° , we detected the strongest spectra at UHF of 15° (Figure 2) Significant observations of collapse occurred at all HF pointing angles, 7° , 11° , and 14° , with UHF of 15° with stronger intensity collapses were detected at 11° , and 14° and UHF of 15° . When the UHF angle was 6° , most of collapse while weak was more observable. We typically observed the coexistence spectra at HF of 7° , 11° , and 14° and UHF of 15° (Figure 3). When HF pointing angles were 11° , and 14° , strong coexistence were detected at UHF of 15° and 12° . When the HF pointing angle was 7° , weak coexistence was detected at UHF of 15° but missing at UHF of 6° . When the HF pointing angle was 7° , there were some strong OPLs for UHF pointing of 15° ; however, most of observations were weak or not detected at UHF of 12° and 6° . When the HF angle was 11° , there was detection of OPL with strong intensity at UHF at 15° for most of the observations, and at UHF of 12° sometimes. OPLs at all HF pointing angles were rarely detected at UHF of 15° .

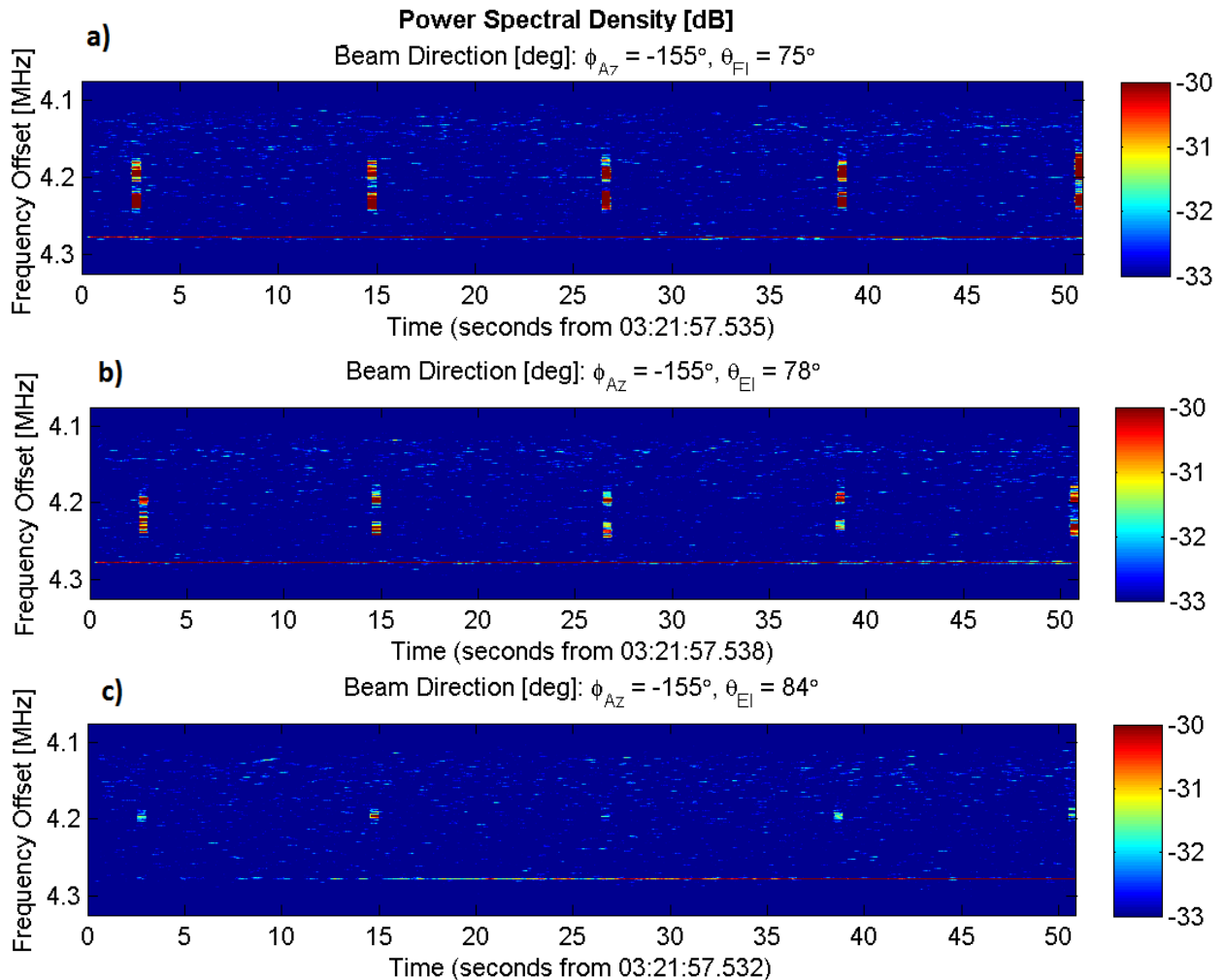


Fig. 2: Spectra for HF at 7° and a) UHF at 15° , b) UHF at 12° , and c) UHF at 6° from 03:21:57 UT to 03:22:47 UT. Cascade lines were observed at UHF of 15° , 12° and 6° . Strong cascades were observed at HF of 7° although most of the cascades were missing at UHF of 6° . Strong and broad spectrum width was observed when UHF was 15° . Cascade lines were stronger at UHF of 15° than UHF of 12° . At UHF of 6° most of cascades were missing.

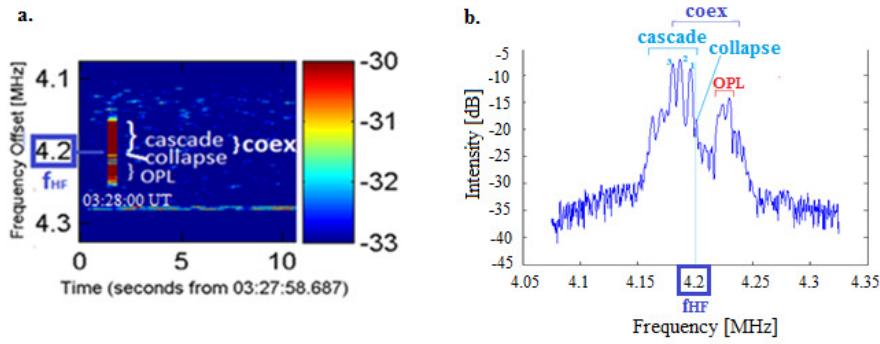


Fig 3 a. Power Spectral Density (PSD) of echo of the instabilities that MUIR detected. HF of 11° and UHF of 15° at 03:28:00 UT on July 25, 2011. **b.** 2-D Intensity of the PSD of shown in Fig 3a showing spectral features associated with SLT.

4. DISCUSSION

Figure 4 shows the electric field line \mathbf{E} , of the pump wave at launched at the aspect angles often chosen in these experiments. The strongest spectra for each HF pointing angle were observed for UHF view angle of 15° corresponding to the geomagnetic field direction. This may be expected due to the refraction of the HF from its launch angle to the respective aspect near reflection. These observations demonstrate both the importance of HF refraction and of the most-favorable UHF radar viewing angles.

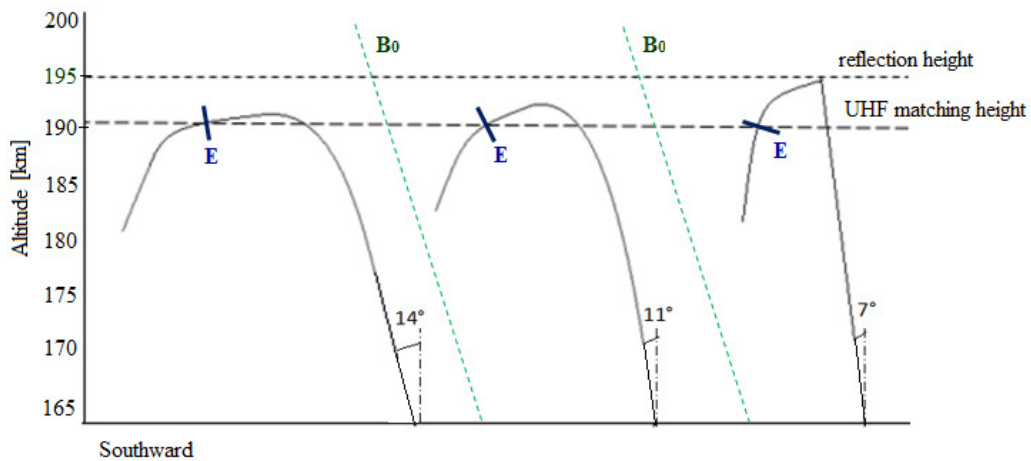


Fig 4. Schematic diagram of the HF pump wave with 7°, 11°, and 14° of the HF pointing angle. The HF pump wave was transmitted with 4.2 MHz at HAARP in Gakona, Alaska (latitude 62° N). The reflection height and UHF matching height are shown as dashed dotted lines. The green dashed dotted line shows the geomagnetic field, \mathbf{B}_0 , and the blue line shows the electric field, \mathbf{E} , of reflection of the HF pump wave.

5. CONCLUSIONS

High power HF transmissions in the O-mode may generate, Langmuir turbulence including caviton collapse, cascade of the LDI and OPL depending on the aspect angle of the HF pointing. The observability of these features also depends strongly on the UHF radar look angle. The high time resolution of the UHF radar, 3.3 ms, allowed observation of the evolution of the SLT. Our *simultaneous* observations at three UHF pointing angles for a range of HF pointing angles

demonstrate for the first time, all of these features may be in turn dominant depending on the chosen HF pointing and UHF observing angles. There were high contrast detections of cascade, collapse, coexistence, and OPL at UHF view angle of 15° with HF pointing angle of 7° , 11° , and 14° . These results demonstrate the effect of refraction of the HF pump electric field into a radar favorable geometry as well as the magnetic zenith effect, a strong echo when the UHF radar angle is close to the magnetic zenith angle described by Rietveld et al., 2003. These observations confirm the existing theory and simulation results of Strong Langmuir Turbulence for RF ionospheric interaction experiments.

ACKNOWLEDGEMENTS

The authors wish to thank the manifold assistance of the HAARP operators especially Michael McCarrick. We thank Paul Bernhardt, Stanley Briczinski, Robert Moore and Mark Golkowski for their support in many aspects of the experiments. We also thank Edward Kennedy for his unflagging efforts to make these experiments a success.

REFERENCES

- Ashrafi, M., M. J. Kosch, K. Kaila, B. Isham, J. Geophys Res. 112 (A5), A05314 (2007)
- Bernhardt, P. A. , L. M. Duncan, C. A. Tepley, R. A. Behnke, J. P. Sheerin, Adv. Space. Res. 8 (1), 271 – 277 (1988).
- Cheung, P. , E. Mjølhus, D. DuBois, J. Pau, H. Zwi, and A. Wong, Phys. Rev. Lett., 79 (7), 1273 – 1276 (1997).
- DuBois, D. F., H. A. Rose, D. Russell, Phys. Rev. Lett., 66 (15) 1970 – 1973 (1991).
- DuBois, D. F., Alfred Hansen, Harvey A. Rose, David Russell, Phys. Fluids. 5 (7) 2616 – 2622 (1993).
- DuBois, D. F., David Russell, Harvey A. Rose, Phys. Plasmas 2, 76 10.1063/1.871119 (1995).
- DuBois, D. F., D. A. Russell, P. Y. Cheung, M. P. Sulzer, Phys Plasmas , 8 (3), 791 – 801 (2001).
- Duncan, L. M., J. P. Sheerin, J. of Geophys. Res., 90(A9), 8371 – 8376 (1985).
- Forme, F. R. E., D. Fontaine, Ann. Geophysicae 17, 182 – 189 (1999).
- Hanssen, A. , E. Mjølhus, D. F. DuBois, H. A. Rose, Journal of Geophysical Research, 97, 12073-91 (1992).
- Isham, B. , C. La Hoz, H. Kohl, T. Hagfors, T. B. Leyser, M. T. Rietveld, J. Atmos. Terr. Phys., 58, 369-384 (1996).

- Isham, B., M. T. Rietveld, T. Hagfors, C. La Hoz, E. Mishin, W. Kofman, T. B. Leyser, A. P. van Eyken, *Adv. Space Res.*, 24(8) 1003 – 1006 (1999).
- Isham, B., T. Hagfors, B. Khudukon, R. Yu. Yurik, E. D. Tereshchenko, M. T. Rietveld, V. Belyey, M. Grill, C. La Hoz, A. Brekke, C. Heinselman, *Ann. Geophys.*, 23 55 – 74 (2005).
- Isham, B., M. T. Rietveld, P. Guio, F. R. E. Forme, T. Grydeland, E. Mjølhu, *Phys. Res. Lett.*, 108 (2012).
- Rietveld, M. T., H. Kohl, H. Kopka, P. Stubbe, *J. Atmos. Terr. Phys.*, 55 577 – 599 (1993).
- Rietveld, M. T., B. Isham, H. Kohl, C. La Hoz, T. Hagfors, *J. of Geophys. Res.*, 105 (A4), 7429 (2000).
- Rietveld, M. T., *J. of Geophys. Res.*, 108 (A4) (2003).
- Rietveld, M. T., M. J. Kosch, N. F. Blagoveshchenskaya, V. A. Kornienko, T. B. Leyser, T. K. Yeoman, *J. Geophys. Res.*, 108 (A4) 1141 (2003).
- Sheerin, J. P., J.C. Weatherall, D.R. Nicholson, G.L. Payne, M.V. Goldman, P.J. Hansen (1982), *J. Atmos. Terr. Phys.*, 44 (12), 1043 – 1048.
- Sheerin, J. P., J. M. Parzych, J. P. Mills, W. A. Bristow, K. M. Groves, American Geophysical Union, Fall Meeting #SA12B-1092 (2003).
- Walker, J. C. G., *Rev. Geophys.*, 17(4), 534 (1979).
- Watanabe, N., M. Golkowski, J. P. Sheerin, and B. J. Watkins, *Earth, Moon, Planets* [in press, 2015]